

## Electronic-structure study of RuS<sub>2</sub>

Ying-Sheng Huang

*Department of Electronic Engineering, National Taiwan Institute of Technology, Taipei, Taiwan 10772, Republic of China*

Yang-Fang Chen

*Department of Physics, National Taiwan University, Taipei, Taiwan 10762, Republic of China*

(Received 30 November 1987; revised manuscript received 21 March 1988)

We report an electrolyte-electroreflectance (EER) study of a RuS<sub>2</sub> single crystal in the energy range 1.9–5.1 eV. The EER spectrum exhibits sharp structure in the vicinity of interband transitions. Transition energies are determined accurately. Photocurrent versus wavelength measurements show an indirect band gap of 1.38 eV. Combining the results of the EER and photocurrent measurements, we construct a possible energy-band structure. It is proposed that RuS<sub>2</sub> has a completely filled 4d *t*<sub>2g</sub> band occupied by six electrons in the low-spin configuration, separated from empty S 3*p* σ\* and Ru 4d *e*<sub>g</sub>\* bands, and the bottom of the conduction band corresponds to the S 3*p* σ\* antibonding states, in agreement with the calculation of Holzwarth *et al.*, but contradicting the assumption of several other authors.

### INTRODUCTION

RuS<sub>2</sub> belongs to the family of transition-metal dichalcogenides crystallizing in the pyrite structure.<sup>1</sup> The semiconducting behavior of this diamagnetic compound was verified by Hulliger<sup>2</sup> on polycrystalline samples. Recently it has been the subject of much interest due to its potential application in energy-related technologies.<sup>3,4</sup> It is a promising material for the thermal catalytic processing of organic sulfur and nitrogen compounds in petroleum refining.<sup>5</sup> It also has interesting photoelectrochemical behavior,<sup>6–8</sup> and photochemical catalytic properties.<sup>9</sup> Despite its technological importance, the theoretical and experimental understanding of its solid-state properties is still relatively incomplete.<sup>10,11</sup>

The energy band structure is one of the most important factors in determining the solid-state properties of a material. The electrolyte-electroreflectance (EER) technique has been proved to be a very powerful tool in the study of the band structure of semiconductors.<sup>12,13</sup> It possesses the advantage of providing a spectrum with sharp features at precise energies, in contrast to the weak and poorly resolved corresponding features in the unmodulated spectra. The only previously published EER spectrum of RuS<sub>2</sub> (Ref. 14) covers a limited range, 2.0–3.1 eV, and no detailed analysis of the spectrum was attempted. In this report we present the EER spectrum of a RuS<sub>2</sub> single crystal in the range 1.9–5.1 eV. Sharp features are observed in the vicinity of interband transitions. The wavelength dependence of the photocurrent is utilized to determine the band gap of the material. By comparing our results with recent band-structure and density-of-states calculations,<sup>10</sup> several interband transitions are identified. Our results are in good agreement with x-ray photoemission measurements<sup>10</sup> and other works,<sup>14</sup> in the measured spectral range. However, we observed several features which were not detected by x-ray photoemission

measurements. Details of these results are presented and discussed in this paper.

### EXPERIMENTAL DETAILS

#### Preparation and properties of RuS<sub>2</sub> crystals

Large single crystals of RuS<sub>2</sub> up to 3×3×3 mm<sup>3</sup> with mirrorlike surfaces have been grown by an "oscillating chemical vapor transport method"<sup>15</sup> using ICl<sub>3</sub> as transport agent. Prior to crystal growth a powdered compound was prepared from the elements (Ru, 99.95% pure; S, 99.9998% pure) by reaction at 1070 °C for 10 d in an evacuated quartz ampoule. The chemical reaction is strongly exothermic. Therefore, the elements had to be heated progressively and very slowly. The lattice parameters of the single crystals have been determined by x-ray powder analysis and the pyrite-type crystal structure has been confirmed. The (111) face appears to be the predominant growth face. Hall effect measurements showed *n*-type semiconducting behavior with electron concentrations between 2×10<sup>17</sup> and 8×10<sup>17</sup> cm<sup>-3</sup>. The electron mobility was found to be approximately 300 cm<sup>2</sup>/V s at room temperature.

#### EER measurements

Although the EER method has been described extensively in the literature,<sup>12,13</sup> the experimental setup used in our present investigations incorporates a number of modifications to improve the accuracy of the measurement, as well as fast data acquisition and processing. The details of the present experimental setup have been described elsewhere.<sup>16</sup> The detector response to the dc component of the reflected light is kept constant by an electric servo mechanism so that the ac reflectance is a direct measure of Δ*R*/*R*, the differential reflectivity.

Scans of  $\Delta R/R$  versus wavelength are obtained using a 0.2-m McPherson grating monochromator together with an Oriel 150-W xenon arc lamp as a monochromatic light source. Phase-sensitive detection is used to measure the differential reflectivity.

The  $\text{RuS}_2$  electrodes were prepared by passing a copper wire through a glass tube and soldering the free end to one end of a copper plate. The crystal was cemented to the copper plate with silver conducting paint. The wire and plate were then insulated with epoxy cement leaving only one face of the crystal exposed to the electrolyte, a 1N  $\text{H}_2\text{SO}_4$  aqueous solution. The counter electrode was a 5-cm<sup>2</sup> platinum plate. To verify that measurements were performed in the low-field regime, EER was performed at  $V_{\text{dc}}=0$  with various ac modulation voltages. The results indicate that the line shape remains invariant for  $V_{\text{ac}} \leq 1$  V (peak to peak) and the amplitude of  $\Delta R/R$  varies linearly with modulation voltage. Dependence of the EER spectra on dc bias voltage was also checked. The amplitude and line shape of EER features remained constant at different bias voltages. Subsequently a 200-Hz square wave was used to modulate the electric field with amplitude 0.4 V peak to peak at  $V_{\text{dc}}=0$ .

#### Photocurrent measurements

The  $\text{RuS}_2$  electrodes were prepared as described above. Teflon test cells were equipped with quartz flat windows. The active crystal face was placed 1 mm from the window to minimize light absorption by the solution. The counter electrode was a 5-cm<sup>2</sup> Pt plate. The electrolytic solution was 1N  $\text{H}_2\text{SO}_4$ . The light source was a 1000-W tungsten halogen lamp (Oriel Corporation). The beam was chopped at 35 Hz with a mechanical chopper and then focused on the entrance slit of 0.2-m McPherson model 270 grating monochromator. Both the entrance and exit slit widths were set to 0.1 mm; part of the exit slit was masked to define a spot of 1 mm height as focused on the electrode face. An Oriel LP 470 filter which cuts off wavelengths shorter than 5000 Å was used to eliminate second-order light at the longer wavelengths. Photoresponse spectra under short-circuit conditions were obtained by connecting the two electrodes to a Stanford Research model 510 lock-in amplifier. Light intensities were measured with a calibrated United Detector Technology model-255 silicon detector. The spectra were corrected for the number of photons reaching the cell at the various wavelengths and normalized to unity at their maxima. Corrections for solution light absorption and the reflection losses at the interfaces were not made.

## RESULTS

The EER spectrum of  $\text{RuS}_2$  at room temperature in the range of 1.9–5.1 eV is shown in Fig. 1. Sharp structure is apparent in the vicinity of interband transitions, as indicated by the small arrows in Fig. 1. By fitting with the

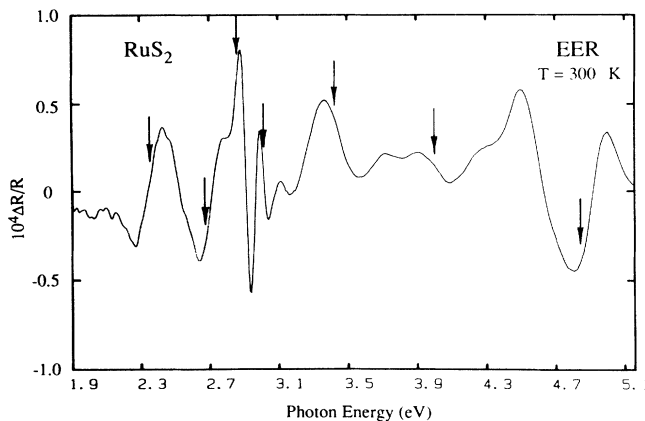


FIG. 1. EER spectrum of  $\text{RuS}_2$

Aspnes third derivative line-shape expression,<sup>17</sup> we can determine the position of the interband transitions to an accuracy better than 5 meV. Table I shows the energy positions of interband transitions obtained from the EER spectrum.

The wavelength dependence of the relative photocurrent is shown in Fig. 2. Here the relative photocurrent is proportional to the short circuit current time photon energy  $h\nu$ . The relative photocurrent increases from 900 to 520 nm and then decreases in the short wavelength region. Two peaks appear around 2.4 and 2.6 eV, as indicated by the small arrows. The indirect band gap of  $\text{RuS}_2$  can be determined from a plot of the square root of relative photocurrent versus  $h\nu$  in the near band edge region.<sup>18</sup> As shown in Fig. 3, the square root of the relative photocurrent depends linearly on  $h\nu$  throughout an extended spectral range. This indicates an indirect transition with a band edge at the intercept of this plot. The band gap derived from this figure is about 1.38 eV.

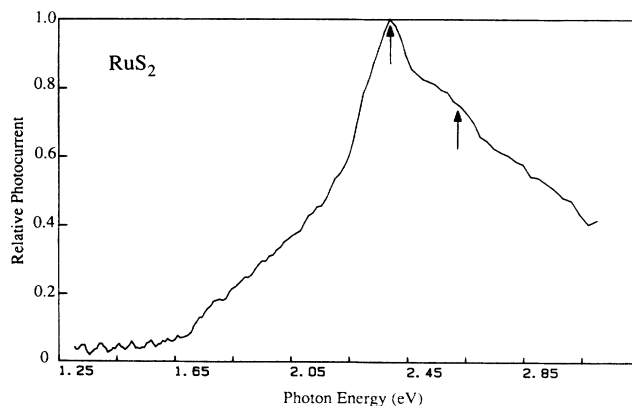


FIG. 2. Relative photocurrent spectrum for single-crystal  $\text{RuS}_2$  in 1N  $\text{H}_2\text{SO}_4$ .

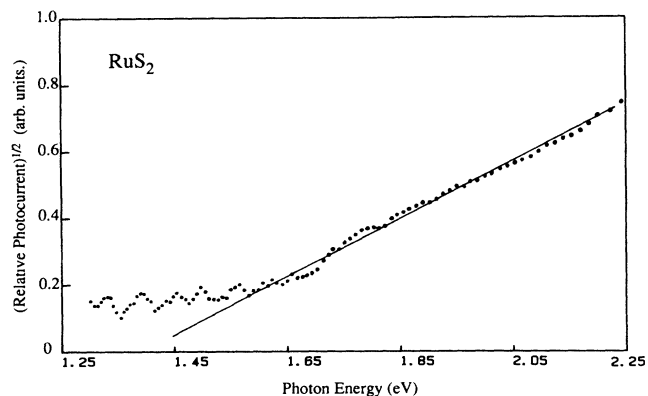


FIG. 3. Square root of relative photocurrent, plotted as a function of photon energy, determines indirect band gap of RuS<sub>2</sub>.

### DISCUSSION OF RESULTS

In the pyrite structure each Ru<sup>2+</sup> ion is surrounded by six S<sub>2</sub><sup>2-</sup> molecules with the site symmetry represented by S<sub>6</sub>. The octahedral component of the ligand field causes metal *d* levels to be split into triply degenerate *t*<sub>2g</sub> and doubly degenerate *e*<sub>g</sub> components.<sup>19</sup> The *t*<sub>2g</sub> and *e*<sub>g</sub> degeneracies are removed by the strong octahedral crystal field of the S<sub>2</sub><sup>2-</sup> ions. The *t*<sub>2g</sub> orbitals orient themselves away from the Ru—S bonding directions and are essentially nonbonding. The *e*<sub>g</sub> orbitals, on the other hand, orient themselves along the Ru-S bonding directions and hybridize with the S 3*p* levels. This hybridization occurs in such a way as to preserve the level structure of the S 3*p* bands of the hypothetical S<sub>2</sub><sup>2-</sup> material. The antibonding (Ru *e*<sub>g</sub><sup>\*</sup>)-(S 3*p* σ<sup>\*</sup>) hybrid states form conduction bands. In general, the conduction bands are strongly hybridized with each other.

In order to analyze our experimental results, we have made use of recent theoretical works<sup>10,20</sup> as well as past experimental studies of related materials such as FeS<sub>2</sub>.<sup>21</sup> Except for the work of Holzwarth *et al.*,<sup>10</sup> all previous studies of RuS<sub>2</sub> assume that the band structure of RuS<sub>2</sub> is the same as that of FeS<sub>2</sub>. Shown in Fig. 4 is the band structure scheme of FeS<sub>2</sub> from Ref. 20. A very broad band mainly of sulfur 3*p* character is superposed on a narrow band derived from the metal *t*<sub>2g</sub> levels. The empty conduction band has mainly iron 3*d* *e*<sub>g</sub><sup>\*</sup> character with some sulphur 3*p* σ<sup>\*</sup> mixing. An energy gap of 0.9 eV separates the occupied iron 3*d* *t*<sub>2g</sub> manifold from the unoccupied iron 3*d* *e*<sub>g</sub><sup>\*</sup> states. Schlegel *et al.*<sup>21</sup> have measured the reflectivity spectrum of FeS<sub>2</sub> and shown that there is a constant splitting of 0.6±0.05 eV of all maxima in the energy range between 1 eV and at least 8.5 eV. This splitting was attributed to a splitting of the final state *e*<sub>g</sub><sup>\*</sup> due to the S<sub>6</sub> site symmetry of the Fe ions. Shown in Fig. 5 is the total density of states for RuS<sub>2</sub> from Ref. 10. The effect of the crystal-field splittings of the *d* electron states into *t*<sub>2g</sub> and *e*<sub>g</sub> bands is indicated. The Ru 4*d* *t*<sub>2g</sub> band is just below the Fermi level and has a width of 1.6 eV. The bonding (S 3*p*)-(Ru 4*d* *e*<sub>g</sub>) band has a width of 5.3 eV and a maximum energy of -1.8

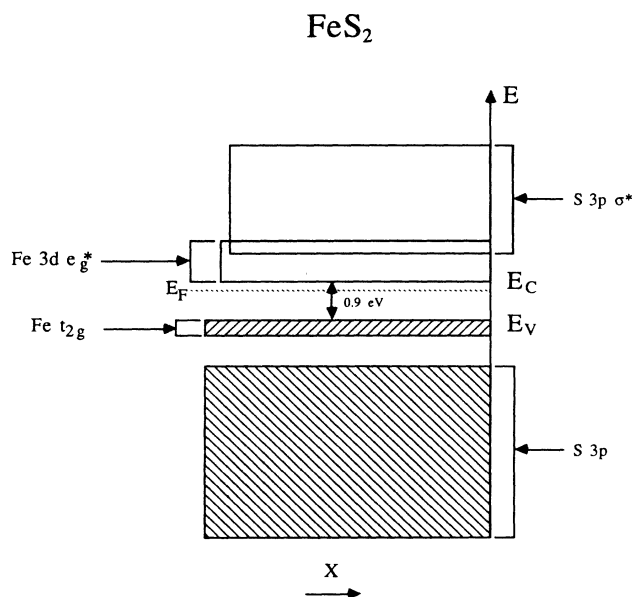


FIG. 4. The band-structure scheme of FeS<sub>2</sub> from Ref. 20.

eV. The unoccupied antibonding (S 3*p* σ<sup>\*</sup>)-(Ru 4*d* *e*<sub>g</sub><sup>\*</sup>) band has a minimum energy of 0.84 eV above *E*<sub>F</sub> and has a width of 4.6 eV. However, Holzwarth *et al.*<sup>10</sup> have pointed out that their calculations tend to underestimate the band gap. The main difference between the band structure reported by Holzwarth *et al.*<sup>10</sup> for RuS<sub>2</sub> and that for FeS<sub>2</sub> is the relative position of the Γ<sub>1</sub><sup>-</sup> state of the

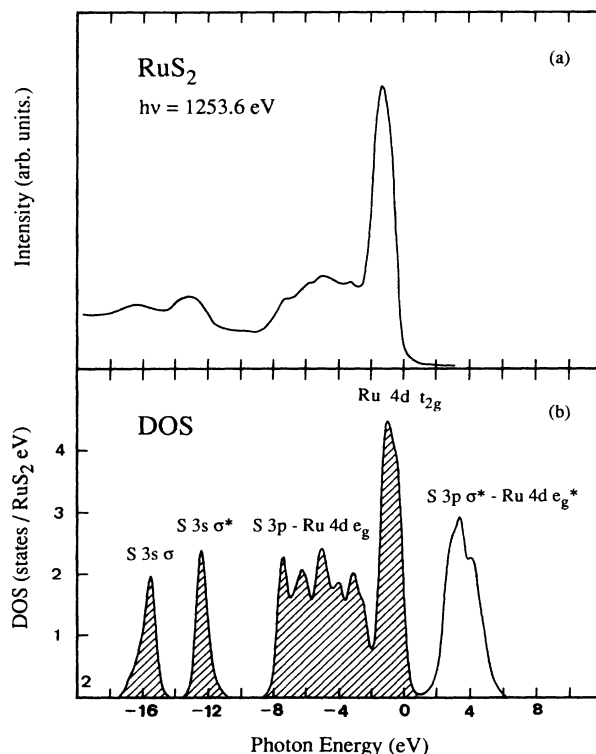


FIG. 5. (a) Experimental density of states of RuS<sub>2</sub> and (b) theoretical density of states of RuS<sub>2</sub> from Ref. 10.

conduction band which corresponds to the S 3p  $\sigma^*$  antibonding molecular orbital.

The value of the band gap of RuS<sub>2</sub> has been the subject of much controversy in recent years.<sup>11</sup> Originally a figure of 1.8 eV was accepted, based on diffuse optical reflection measurements on powdered samples.<sup>2</sup> From optical absorption measurements Bichsel *et al.*<sup>22</sup> estimated the energy gap of single-crystal RuS<sub>2</sub> at 1.3 eV. Attempts to determine the energy gap using the photoresponse spectra at semiconductor-electrolyte interfaces were also inconclusive. Guittard *et al.*<sup>23</sup> first observed such a photoresponse spectrum using sintered RuS<sub>2</sub> electrodes, and suggested a value of 1.3–1.5 eV. However, in later work from the same laboratory, on single-crystal electrodes, the value obtained was 1.85 eV.<sup>8</sup> Nonetheless, in published spectra,<sup>24</sup> a significant response to photons of energy below 1.8 eV is remarkably persistent at single-crystal surfaces. An even stronger photoresponse at the red end of the spectrum was observed using sintered electrodes<sup>4</sup> and was interpreted in terms of donor levels close to the Fermi level and associated with structural defects in the material. However, the effect could also be interpreted in terms of an indirect energy gap of around 1.4 eV with a low transition cross section, followed by a higher gap of 1.8 eV. Our results indicate that the lower value might be correct. In order to obtain more accurate results, the relative photocurrent should be corrected by taking account of reflectance losses at the interfaces and absorption losses in the electrolyte. The indirect energy gap of 1.38 eV is much larger than the theoretical value of 0.84 eV.<sup>10</sup> The discrepancy between the theoretically calculated density of states and our experimental results can be resolved if the theoretical band gap is increased by about 0.5 eV.

EER measurements in RuS<sub>2</sub> were recently performed by Herm *et al.*<sup>14</sup> in the range of 2.0–3.1 eV. Their EER spectrum also shows sharp features at around 2.45 and 2.9 eV, consistent with our results, but no detailed analysis was made. Comparing our results with the work of Holzwarth *et al.*,<sup>10</sup> it is possible to associate the features of the EER spectrum with the appropriate interband transitions. We can relate the features at 2.35, 2.68, 2.87, and 3.02 eV to the transitions from Ru 4d  $t_{2g}$  non-bonding states to the antibonding (Ru  $e_g^*$ )-(S 3p  $\sigma^*$ ) hybrid states. The structure at higher energies from 3.4–5.1 eV is mainly due to interband transitions from states of largely S 3p character to (Ru  $e_g^*$ )-(S 3p  $\sigma^*$ ) hybrid states. A band-structure scheme consistent with the transition energies shown in Table I is constructed in Fig. 6.

Comparing the relative photocurrent and EER spectra, the 2.4- and 2.6-eV peaks in the relative photocurrent spectrum occur at almost the same energy as the first two features in the EER spectrum. These photocurrent peaks may indicate the strong absorption of the direct interband transitions around the critical points.

There is additional evidence showing that our results agree with the band structure calculated by Holzwarth *et al.*,<sup>10</sup> in which the bottom of the conduction band is the  $\Gamma_1^-$  state corresponding to the S 3p  $\sigma^*$  antibonding molecular orbital. We did not observe a constant split-

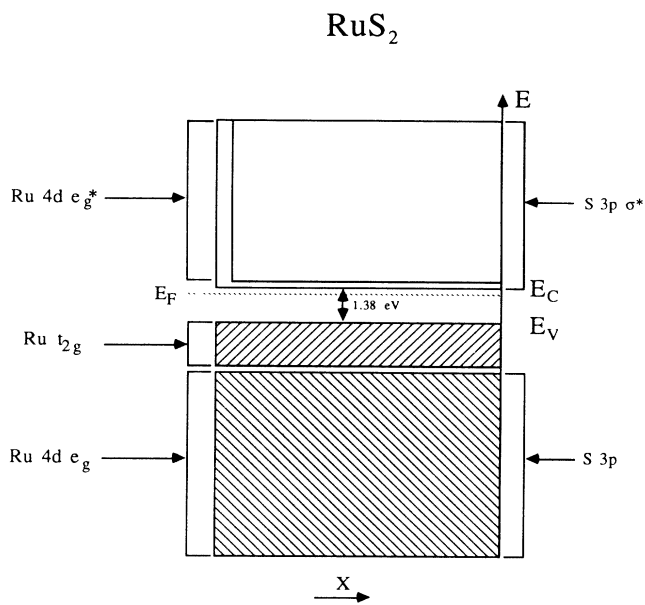


FIG. 6. Energy-level scheme of RuS<sub>2</sub>

ting of all interband transitions in the measured energy range as reported by Schlegel *et al.*<sup>21</sup> for FeS<sub>2</sub>, which may indicate that the bottom of the conduction band does not correspond to the Ru 4d  $e_g^*$  antibonding states. In the study of the photoelectrochemical evolution of oxygen with the RuS<sub>2</sub> electrode,<sup>25</sup> we have observed that the RuS<sub>2</sub> crystal shows clear evidence of corrosion after 20 h of photochemical oxidation by white light in 1N H<sub>2</sub>SO<sub>4</sub> at 1.0 V with respect to the saturated calomel electrode (see Fig. 7). This result can be related to the fact that the excitations are from Ru 4d  $t_{2g}$  to the S 3p  $\sigma^*$  antibonding molecular orbital, which tend to weaken the S—S bond in the pyrite structure, rather than  $d-d$  transitions. Transition-metal dichalcogenides such as MoS<sub>2</sub> and WS<sub>2</sub>, in which the lowest-energy interband transitions are primarily intra-atomic  $d-d$  transitions,<sup>26,27</sup> make stable photoelectrochemical electrodes. In these materials, in contrast to RuS<sub>2</sub>, the photoelectrochemical

TABLE I. Energy positions of various features observed in the EER spectrum of RuS<sub>2</sub> (see Fig. 1) and our assignment of the interband transitions.

RuS <sub>2</sub> (eV)	The assignment of interband transitions
2.35	Ru $t_{2g}$ → S 3p $\sigma^*$
2.68	Ru $t_{2g}$ → Ru $e_g^*$ + S 3p $\sigma^*$
2.87	Ru $t_{2g}$ → Ru $e_g^*$ + S 3p $\sigma^*$
3.02	Ru $t_{2g}$ → Ru $e_g^*$ + S 3p $\sigma^*$
3.43	S 3p → Ru $e_g^*$ + S 3p $\sigma^*$
4.12	S 3p → Ru $e_g^*$ + S 3p $\sigma^*$
4.85	S 3p → Ru $e_g^*$ + S 3p $\sigma^*$



FIG. 7. SEM picture of a RuS<sub>2</sub> single crystal after 20 h of photochemical oxidation by white light in 1N H<sub>2</sub>SO<sub>4</sub> at 1.0 V with respect to the saturated calomel electrode.

reaction does not attack the metal-sulfur chemical bonds and therefore photocorrosion occurs less readily.

Comparing our results with x-ray photoemission measurements,<sup>10</sup> the features at around 2.9 and 4.9 eV are in

good agreement if the band gap is extended by about 0.5 eV. The other features in the EER spectrum are absent in the x-ray photoemission spectrum. This can be explained by the poorer energy resolution and lower sensitivity to weak spectral features of the x-ray photoemission technique.

## CONCLUSIONS

EER and photocurrent measurements have been carried out in an RuS<sub>2</sub> single crystal. The EER spectrum exhibits sharp structure in the vicinity of interband transitions, while the photoresponse spectrum shows an indirect band gap of 1.38 eV. Thus a possible energy band structure is constructed. It is proposed that RuS<sub>2</sub> has a completely filled 4d *t*<sub>2g</sub> band occupied by six electrons in the low spin configuration, separated 1.38 eV from empty S 3p  $\sigma^*$  and Ru 4d *e*<sub>g</sub><sup>\*</sup> bands. The bottom of the conduction band corresponds to the S 3p  $\sigma^*$  antibonding states, leading to partial decomposition of RuS<sub>2</sub> crystals under certain photoelectrochemical conditions.

## ACKNOWLEDGMENTS

This work was supported by the National Science Council of the Republic of China under Contracts No. NSC75-0208-M011-01 and No. NSC77-0208-M011-01.

- <sup>1</sup>O. Sutarno, O. Knop, and K. I. G. Reid, *Can. J. Chem.* **45**, 1391 (1967).
- <sup>2</sup>F. Hulliger, *Nature (London)* **200**, 1064 (1963).
- <sup>3</sup>R. Guittard, R. Heindl, R. Parsons, A. M. Redon, and H. Tributsch, *J. Electroanal. Chem.* **111**, 401 (1980).
- <sup>4</sup>A. M. Redon, *Solar Cells* **15**, 27 (1985).
- <sup>5</sup>T. A. Pecoraro and R. R. Chianelli, *J. Catal.* **67**, 430 (1981).
- <sup>6</sup>H. M. Kuhne and H. Tributsch, *J. Electrochem. Soc.* **130**, 1448 (1983).
- <sup>7</sup>R. Heindl, R. Parsons, A. M. Redon, H. Tributsch, and J. Vigneron, *Surf. Sci.* **115**, 91 (1981).
- <sup>8</sup>H. Ezzaouia, R. Parsons, A. M. Redon, H. Tributsch, and J. Electroanal. Chem. **145**, 279 (1983).
- <sup>9</sup>D. H. M. W. Thewissen, E. A. Van der Zouwen-Assink, K. Timmer, A. H. A. Tinnemans, and A. Mackor, *J. Chem. Soc., Chem. Commun.* **14**, 941 (1984).
- <sup>10</sup>N. A. W. Holzwarth, Suzanne Harris, and K. S. Liang, *Phys. Rev. B* **32**, 3745 (1985).
- <sup>11</sup>A. J. McEvoy, *Mater. Chem. Phys.* **14**, 113 (1986).
- <sup>12</sup>D. E. Aspnes, in *Handbook of Semiconductors*, edited by M. Balkanski (North-Holland, Amsterdam, 1980), Vol. 2, p. 109.
- <sup>13</sup>Fred H. Pollak, *Proc. Soc. Photo-Opt. Instrum. Eng.* **276**, 142 (1982).
- <sup>14</sup>D. Herm, H. Wetzel, and H. Tributsch, *Surf. Sci.* **163**, 13 (1985).
- <sup>15</sup>Y. S. Huang and S. S. Lin, *Mater. Res. Bull.* **23**, 277 (1988).
- <sup>16</sup>Y. S. Huang, H. M. Chen, C. J. Chang, and G. J. Jan, *Chin. J. Phys.* **23**, 144 (1985).
- <sup>17</sup>D. E. Aspnes, *Surf. Sci.* **37**, 418 (1973).
- <sup>18</sup>See, for example, J. I. Pankove, *Optical Processes in Semiconductors* (Dover, New York, 1975).
- <sup>19</sup>See, for example, C. J. Ballhausen, *Introduction to Ligand Field Theory* (McGraw-Hill, New York, 1962).
- <sup>20</sup>S. Lauer, A. X. Trautwein, and F. E. Harris, *Phys. Rev. B* **29**, 6774 (1984).
- <sup>21</sup>A. Schlegel and P. Wachter, *J. Phys. C* **9**, 3363 (1976).
- <sup>22</sup>R. Bichsel, F. Levy, and H. Berger, *J. Phys. C* **17**, L19 (1984).
- <sup>23</sup>R. Guittard, R. Heindl, R. Parsons, A. M. Redon, and H. Tributsch, *J. Electroanal. Chem.* **111**, 401 (1980).
- <sup>24</sup>H. Ezzaouia, J. W. Foise, and O. Gorochoy, *Mater. Res. Bull.* **20**, 1353 (1985).
- <sup>25</sup>Y. S. Huang and Y. F. Chen (unpublished).
- <sup>26</sup>H. Tributsch and J. C. Bennett, *J. Electroanal. Chem.* **81**, 97 (1977).
- <sup>27</sup>H. Tributsch, *Struct. Bonding (Berlin)* **49**, 127 (1982).

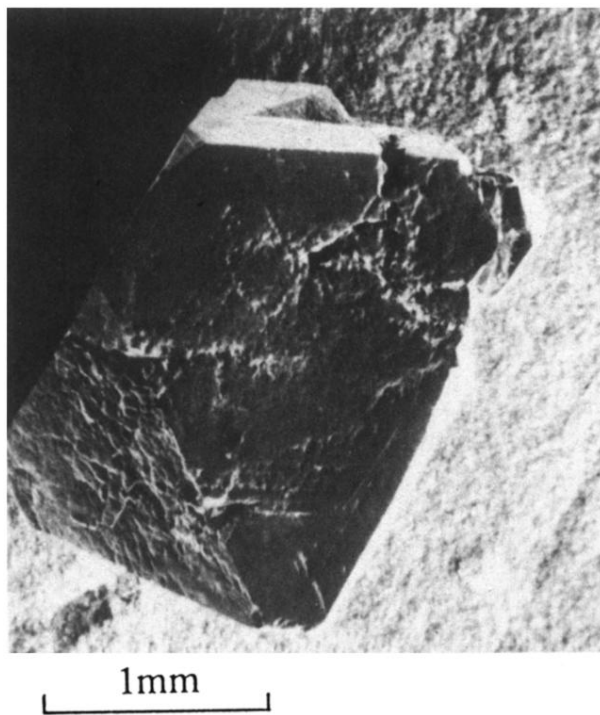


FIG. 7. SEM picture of a RuS<sub>2</sub> single crystal after 20 h of photochemical oxidation by white light in 1*N* H<sub>2</sub>SO<sub>4</sub> at 1.0 V with respect to the saturated calomel electrode.